JCI insight

Altered plasma metabolite levels can be detected years before a glioma diagnosis

Sebastian Löding, … , Benny Björkblom, Beatrice Melin

JCI Insight. 2023. https://doi.org/10.1172/jci.insight.171225.

Research In-Press Preview Metabolism Oncology

Graphical abstract

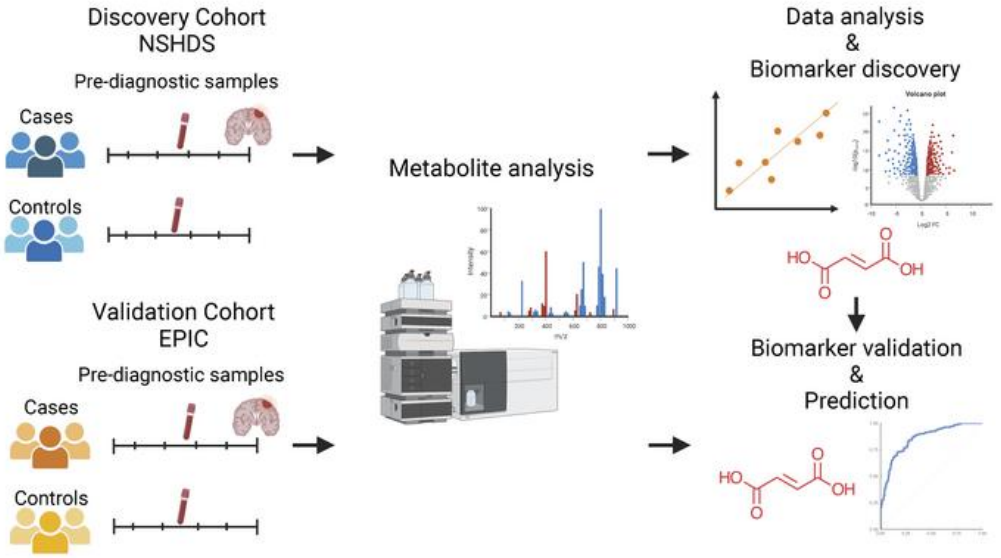

Altered plasma metabolite levels can be detected years before a glioma diagnosis

Sebastian Löding[1], Ulrika Andersson[2,3], Rudolf Kaaks[4], Matthias B. Schulze[5,6], Valeria Pala[7], Ilona Urbarova[8], Pilar Amiano[9,10,11], Sandra M. Colorado-Yohar[9,12,13], Marcela Guevara[9,14,15], Alicia K. Heath[16], Anastasia Chrysovalantou Chatziioannou[17], Mattias Johansson[18], Lars Nyberg[19,20] Henrik Antti[1], Benny Björkblom[1*], Beatrice Melin[3*].

[1] Department of Chemistry, Umeå University, SE-901 87 Umeå, Sweden.

[2] Biobank Reserach Unit, Umeå University, SE-901 87 Umeå, Sweden.

[3] Department of Radiation Sciences, Oncology, Umeå University, SE-901 87 Umeå, Sweden.

[4] Division of Cancer Epidemiology, German Cancer research Center (DKFZ), Heidelberg, Germany.

[5] Department of Molecular Epidemiology, German Institute of Human Nutrition Potsdam-Rehbruecke, Nuthetal, Germany

[6] Institute of Nutritional Science, University of Potsdam, Nuthetal, Germany

[7] Epidemiology and Prevention Unit, Fondazione IRCCS Istituto Nazionale dei Tumori, Milan, Italy

[8] Department of Community Medicine, Faculty of Health Sciences, UiT The Arctic University of Norway, PO Box 6050 Lagnes, 9037 Tromsø, Norway.

[9] CIBER Epidemiología y Salud Pública (CIBERESP), Spain.

[10] Ministry of Health of the Basque Government, Public Health Laboratory in Gipuzkoa, San Sebastián, Spain.

[11] Epidemiology of Chronic and Comunnicable Diseases Area, Biodonostia Health Research Institute, San Sebastián, Spain.

[12] Department of Epidemiology, Murcia Regional Health Council, IMIB, Murcia, Spain.

[13] Research Group on Demography and Health, National Faculty of Public Health, University of Antioquia, Medellín, Colombia.

[14] Instituto de Salud Pública de Navarra, 31003 Pamplona, Spain.

[15] Navarra Institute for Health Research (IdiSNA), 31008 Pamplona, Spain.

[16] Department of Epidemiology and Biostatistics, School of Public Health, Imperial College London, London, United Kingdom.

[17] Nutrition and Metabolism Branch, International Agency for Research on Cancer, 150 Cours Albert Thomas, Lyon, France.

[18] Genomic Epidemiology Branch, International Agency for Research on Cancer, Lyon, France.

[19] Department of Radiation Sciences, Diagnositc Radiology, Umeå Univeristy, SE-901 87 Umeå, Sweden.

[20] Department of Integrative Medical Biology (IMB), Umeå University, SE-901 87 Umeå, Sweden.

*Corresponding authors with equal contribution:

Benny Björkblom, Department of Chemistry, Umeå University, Linnaeus väg 10, SE-901 87 Umeå, Sweden. +46907866230, benny.bjorkblom@umu.se

Beatrice Melin, Department of Radiation Sciences, Oncology, Umeå University. SE-901 87 Umeå, Sweden +46730918028, beatrice.melin@umu.se

Conflict of interest statement: The authors have declared that no conflict of interest exists.

Abstract

Genetic and metabolic changes in tissue and blood are reported to occur several years before glioma diagnosis. As gliomas are currently detected late, a liquid biopsy for early detection could impact the quality of life and prognosis of patients. Here, we present a nested case-control study of 550 pre-diagnostic glioma cases and 550 healthy controls, from the Northern Sweden Health and Disease study (NSHDS) and the European Prospective Investigation into Cancer and Nutrition (EPIC) study. We identified 93 significantly altered metabolites related to glioma development up to eight years before diagnosis. Out of these metabolites, a panel of 20 selected metabolites showed strong disease correlation and consistent progression pattern towards diagnosis in both the NSHDS and EPIC cohorts, and separated favorably future cases from controls independently of biological sex. The blood metabolite panel also successfully separated both lower grade glioma and glioblastoma cases from controls, up to eight years before diagnosis in NSHDS (glioma AUC=0.85, P=3.1e-12; glioblastoma AUC=0.85, P=6.3e-8), and up to two years before diagnosis in EPIC (glioma AUC=0.81, P=0.005; glioblastoma AUC=0.89, P=0.04). Pathway enrichment analysis detected metabolites related to the TCA-cycle, Warburg effect, gluconeogenesis, cysteine-, pyruvate- and tyrosine metabolism as the most affected.

Introduction

Gliomas, the most common type of malignant primary brain tumors, are usually detected late, when patients exhibit severe neurological symptoms such as seizures (1). Although treatment with surgical resection and concomitant radiochemotherapy have improved patient survival, prognosis for glioma patients is still poor. Patients suffering from the most common and most aggressive subtype - glioblastoma - have a median survival time of only 15 months (2). As treatment options are limited, earlier detection of high risk individuals could improve prognosis and impact patient survival (3).

Previous studies have shown that gliomagenesis start several years before clinical symptoms appear (4, 5). Genetic aberrations causing glioblastoma tumorigenesis have been estimated to occur up to seven years before diagnosis (4). Further, a set of fifteen metabolites in blood was associated with glioma progression up to eight years before diagnosis (5), and a set of nine metabolites were associated with higher glioblastoma risk even earlier (6). In both studies, the sets of metabolites indicated an imbalanced redox homeostasis (5, 6). In addition, it is well documented that elevated levels of the mitochondrial tricarboxylic acid (TCA) cycle metabolites fumarate, succinate and D-2-hydroxyglutarate promote tumorigenesis (7).

In this study, we analyzed a large set of pre-diagnostic plasma samples from two independent cohorts, the Northern Sweden Health and Disease study (NSHDS) (8) and the European Prospective Investigation into Cancer and Nutrition (EPIC) study (9), from 18 study centers. The samples were collected 0.2 to 25 years before glioma diagnosis and analyzed together with matched controls by global metabolomics analyses for discovery and validation of metabolic changes related to glioma development.

Results

Data overview

Study overview and description of study participants in the discovery (NSHDS) and validation (EPIC) cohorts are presented in Figure 1, A and B, and Table 1, respectively. For case-control pairing, we employed stringent matching based on sex, BMI, age, time in freezer, fasting status and study center. To obtain an overview of all 1100 analyzed plasma samples from the global mass spectrometry-based metabolomic analyses, we first performed a Uniform Manifold Approximation and Projection for Dimension Reduction (UMAP) analysis (Figure 2, A and B). We included all metabolic features that were in common for both NSHDS and EPIC, in total 802 metabolites (see Supplemental Methods for detailed information on data collection and curation). UMAP plots of all samples, both future glioma cases (n=550) and matched healthy controls (n=550) from EPIC and NSHDS are shown as independent observations in Figure 2A, and as dependent case-control pairs in Figure 2B. As anticipated, we observe cohort- and country specific clusters when analyzing all cases and controls independently (Figure 2A), indicating systematic differences between and within the cohorts. This difference between cohorts and sampling countries was expected since samples were from multiple sampling centers with varying sampling routines and population differences. The study was therefore designed to reduce the impact of pre-analytical differences, by utilizing the differences in relative metabolite concentration between tightly matched case-control pairs. The UMAP plot constructed from an effect matrix of calculated metabolite concentration differences between matched case-control pairs (n=550 pairs) shows that the overlap of samples from the cohorts greatly improves, and less cohort-specific clusters are observed (Figure 2B). This analysis shows the benefit of stringent matching of case-control pairs within the same cohorts,

as a processing step before data analysis, to increase sensitivity for true biomarker detection and decrease both variation and false discoveries originating from pre-analytical differences and covariates.

Metabolites that indicate early glioma development

We used multivariate statistical analysis by means of Orthogonal Projections to Latent Structures – Effect Projection (OPLS-EP) to make use of the effect matrix obtained from matched case-control pairs and to discover metabolites related to glioma development. Since previous studies indicate that gliomagenesis starts up to eight years before diagnosis (4, 5), we initially focused our analysis on case-control pairs sampled up to eight years before diagnosis in NSHDS (n=130 pairs). From the generated OPLS-EP model (CV-ANOVA P=0.005, R^2Y=0.46, Q^2=0.08), 93 metabolites with known identity were found to reach statistical significance (Figure 2C and Supplemental Table 1). Of the 93 significant metabolites found in NSHDS, 87 metabolites were also detected in samples from EPIC. However, in EPIC samples only one of the 87 metabolites, fumarate, reached statistical significance (P=0.02) when focusing on samples collected up to eight years to diagnosis, while cystine was borderline significant (P=0.06). It should be noted that plasma samples from EPIC were collected using sodium citrate as anticoagulant, which has been reported to induce matrix effects and quench metabolite signals (10, 11). Also, the majority of the EPIC samples were collected from non-fasting individuals whereas the majority of the NSHDS samples were from fasting individuals (Figure 1B and Table 1), which could impact metabolite levels (12). However, our earlier study shows that the difference in levels of glioma associated metabolites between cases and controls increases towards diagnosis (5). Therefore, we analyzed the metabolite levels towards diagnosis for the 87 out of 93 significant metabolites that could be detected in EPIC, to examine if the

glioma associated metabolites would be similarly altered closer to diagnosis. This analysis shows that 20 of 87 metabolites displayed the same direction towards diagnosis, with a mean difference of >10% closer to diagnosis (within two years and/or one year to diagnosis), in NSHDS and EPIC (Figure 3 and Table 2). For most metabolites, the levels were higher in cases compared to controls, with the highest levels closest to diagnosis (Figure 3). Except the levels of tyramine O-sulfate, PE(P-16:0/18:2) and PE(P-18:0/18:2), that were lower in cases, with even more reduced levels closer to diagnosis (Figure 3) indicating a reversed molecular function. All significant metabolites for samples collected more than eight years to diagnosis are listed in Supplemental Table 2.

To validate our findings of elevated lactate levels (Table 2 and Figure 3), we used the LC-MS/MS-based Biocrates MxP500 quant platform for targeted identification and quantification of lactate levels in 354 NSHDS samples. Quantified µM levels of lactate were compared with the relative amounts from the Metabolon platform (Supplemental Figure 1, A and B). The methods showed strong correlation (R^2=0.84), with elevated lactate levels in cases within eight years to diagnosis, and even higher levels closer to diagnosis (Supplemental Figure 1B). Lactate levels in samples that were not measured quantitatively were predicted using linear regression (Supplemental Figure 1C). The quantitative targeted measurements of lactate, including predicted levels, showed the same level of significance in case-control pairs within eight years to diagnosis as seen for the untargeted measurement ($P_{untargeted}$ = 0.0004, $P_{targeted}$ = 0.0004).

Predicting glioma development

To assess if the panel of 20 selected metabolites with consistent progression pattern towards diagnosis in both NSHDS and EPIC could predict glioma

development, we first generated an OPLS-EP model using the metabolites and the 130 case-control pairs in NSHDS sampled within eight years to diagnosis. The predictive ability of the model was assessed by predicting the samples from NSHDS, used to generate the model, and samples from EPIC that were not used to generate the model. The results were evaluated with Receiver Operating Characteristic (ROC) analyses (Figure 4). Within eight years to diagnosis, the panel of 20 metabolites predicted case-control pairs in NSHDS well, with an AUC of 0.853 and P=3.1e-12 (Figure 4A) whereas case-control pairs in EPIC showed a poor prediction with an AUC of 0.507 and P=0.88 (Figure 4B). However, prediction limited to case-control pairs within two years to diagnosis in EPIC displayed an AUC of 0.806 with a significant P-value of 0.005 (Figure 4D). Similar results were observed for case-control pairs within two years to diagnosis in NSHDS (AUC=0.816, P-value=0.004) (Figure 4C).

The blood metabolome is very dynamic and affected by many exogenous and biological factors, highlighting the need to minimize confounding variation by study design. As metabolic differences between males and females are obvious in blood samples, we wanted to assess our strategy and the predictive ability of the 20-metabolite panel on females and males separately. Also, here the panel predicted both female and male case-control pairs in NSHDS well, with AUC values for females of 0.870 and P=3.4e-9 (Figure 5A) and AUC values for males of 0.818 and P=2.1e-4 (Figure 5D). Prediction limited to case-control pairs within two years to diagnosis in NSHDS and EPIC displayed also solid AUC values for both females and males (Figure 5, B-F), with the best prediction of males in EPIC within two years of diagnosis (AUC=0.964, P=6.1e-4). To further assess the predictive ability of the panel on different glioma subtypes, ROC analyses were performed on glioblastoma and all other gliomas (non-glioblastoma) separately. Case-control pairs within eight and two years to diagnosis from NSHDS and within two years from EPIC were predicted (Figure 6).

The panel performed well and gave slightly better predictions for glioblastoma, with AUCs of 0.851 and 0.813 in NSHDS within eight and two years, respectively, and AUC of 0.890 in EPIC within two years to diagnosis (Figure 6, A-C). Predictions of non-glioblastoma were also good with AUCs of 0.832 and 0.785 in NSHDS within eight and two years, respectively, and AUC of 0.702 in EPIC within two years to diagnosis (Figure 6, D-F). However, the predictions of non-glioblastoma within two years in NSHDS and EPIC did not reach statistical significance, likely due to small sample sizes.

Due to coherent results of detecting glioma development within two years to diagnosis in NSHDS and EPIC, we calculated the significance for metabolites within two years to diagnosis in case-control pairs from both cohorts. 17 of the 93 significant metabolites within eight years to diagnosis were still significant within two years to diagnosis in NSHDS (Supplemental Figure 2A and Supplemental Table 3), whereas three were found significant within two years to diagnosis in EPIC (Supplemental Figure 2B and Supplemental Table 4).

Altered metabolic pathways

We performed a metabolite enrichment analysis to put the panel of 20 metabolites in common, and the 93 significant metabolites discovered in NSHDS into biological context. For the 93 significant metabolites, the most significant overrepresented metabolic pathways were the TCA cycle (P=0.002) and the Warburg effect (P=0.01) (Figure 7A). Other significantly overrepresented pathways (P<0.05) were pyruvate- and cysteine metabolism, gluconeogenesis, and tyrosine metabolism. In the panel of 20 metabolites with consistent metabolite level differences in NSHDS and in EPIC closer to diagnosis, were the Warburg effect (P=0.02), pyruvate metabolism (P=0.03) and the TCA cycle (P=0.07) still the most overrepresented pathways (Figure 7B). The metabolites within the significant pathways are however

tightly connected. The significant metabolites and pathways, together with neighboring pathway of amino acid metabolism, are presented in Table 3 and Figure 7C. In this analysis, the levels of all significant metabolites within the presented pathways were higher in cases compared to controls. In addition, the levels were even higher towards diagnosis for all metabolites (Supplemental Figure 3).

Finally, we examined the plasma levels of 2-hydroxyglutarate as several endogenously expressed TCA cycle related metabolites were found to be significantly altered. Plasma levels of 2-hydroxyglutarate, the oncometabolite produced by a mutation in isocitrate dehydrogenase, showed elevated levels closer to diagnosis in both NSHDS and EPIC samples (Supplemental Figure 4), but did not reach statistical significance. As isocitrate dehydrogenase mutation is uncommon in glioblastoma, we examined glioblastoma and non-glioblastoma cases separately (Supplemental Figure 4, see Supplemental Methods for classification). Here the plasma levels of 2-hydroxyglutarate followed the same trend as observed for all glioma combined, except for non-glioblastoma in EPIC samples that showed reduced levels towards diagnosis.

Discussion

In this study, we found 93 metabolites in NSHDS with significantly different plasma levels within eight years of glioma diagnosis compared to healthy controls. In addition, 20 of these metabolites displayed consistent metabolite level differences closer to diagnosis in samples from the NSHDS cohort and the multi-center EPIC cohort, with a mean difference of >10% between cases and controls. This panel of 20 metabolites showed good ability to separate future glioma cases from matched controls within eight years to diagnosis in NSHDS, and within two years to diagnosis in EPIC, independent of biological sex or glioma subtype. Our results are in line with previous studies that have detected metabolic alterations in pre-diagnostic plasma samples up to eight years before glioma diagnosis (5), and longitudinal whole-genome profiling of gliomas showing that mutated founder cells with common genetic aberrations emerge up to seven years before diagnosis (4). Metabolites in our panel have previously been linked to tumor metabolism, which in our view strengthens their validity. Our metabolite enrichment analysis particularly highlighted metabolites linked to the TCA cycle pathway and the Warburg effect, as the most affected. Elevated plasma levels of fumarate and cystine were particularly robust in pre-diagnostic cases from both NSHDS and EPIC within eight years to diagnosis.

The TCA cycle was found significantly overrepresented in the enrichment analyses. Elevated levels of TCA cycle-related metabolites; fumarate, succinate and D-2-hydroxyglutarate have previously been linked to oncometabolite-driven tumorigenesis (7). TCA cycle-related metabolites play a central role in the Warburg effect. The Warburg effect is characterized by a metabolic reprogramming, causing an increased rate of glycolysis and production of lactate under aerobic conditions with functioning mitochondria, which is seen in glioma cells and other cancers (13, 14).

Accumulated lactate is released from the cell and acidifies the tumor microenvironment, favoring tumor progression. Here, we report significantly elevated levels of lactate in pre-diagnostic glioma cases within eight years to diagnosis. In addition, we found significantly elevated levels of N-lactoyl valine, N-lactoyl leucine and N-lactoyl phenylalanine within eight years to diagnosis. N-lactoyl amino acid production is catalyzed by reverse proteolysis of lactate and amino acids by carnosine dipeptidase 2 (15). N-lactoyl amino acids are poorly studied, and their role in glioma development and cancer is unknown. Interestingly, seven of the 20 metabolites in our panel (lactate, fumarate, malate, hypoxanthine, N-lactoyl valine, N-lactoyl leucine and N-lactoyl phenylalanine), are some of the most elevated metabolites in blood during physical activity (16, 17). Moreover, exercise-induced N-lactoyl phenylalanine has recently been hypothesized to function as a molecular signal to regulate energy balance (17). Hypothetically, the shared set of metabolites related to glioma development and physical activity may be linked to inflammatory mediators, as elevated levels of inflammatory cytokines have also been reported in pre-diagnostic glioma blood (18). Elevated levels of lactate and hypoxanthine have also been reported in blood of people with immune-mediated inflammatory disease (19). These metabolites may reflect a state of increased energy demand and energy turnover caused by inflammation.

In our analysis, products of the tyrosine metabolism were also found significant, with higher levels of homovanillate and S-adenosylhomocysteine and lower levels of tyramine O-sulfate in pre-diagnostic glioma cases. In the brain, tyrosine is the starting material for synthesis of catecholamines (20). Homovanillate is the end-product of dopamine catabolism, and is elevated in urine of patients with catecholamine-secreting tumors such as neuroblastoma (21). Altered tyrosine metabolism has previously also been found to be related to glioma development, where

elevated plasma levels of 4-hydroxyphenylacetic acid was detected in pre-diagnostic glioma cases (5).

Our findings are also consistent with previous reports of imbalanced redox homeostasis for pre-diagnostic glioma cases, highlighting elevated levels of metabolites such as cystine, cysteine, eryhtritol, erythronate and hypoxanthine (5, 6). However, a complete overlap and replication of significant metabolites between current and the previous studies are not to be expected, as the analyses were performed on different analytical platforms with different metabolite coverages.

As stated, NSHDS and EPIC samples were collected using different blood-anticoagulants and the majority of the participants have different fasting status between the cohorts, which together with the multi-center structure of EPIC introduced variation unrelated to the research question and complicated the validation of discovered metabolites in NSHDS. However, these differences also imply some degree of robustness to our findings, as they were consistent in two largely diverse cohorts.

Our results show that glioma development is detectable in blood up to two years before diagnosis, and even up to eight years before diagnosis in a homogenous sample population such as NSHDS. Other disease studies have shown that blood tests have the potential to detect neurological disorders, such as Parkinson's and Alzheimer's disease, in their early stages (22, 23). Clinically, a blood test for glioma diagnostics could be used for early detection in patients with non-specific symptoms or to discriminate unclear lesions at brain imaging. The panel of 20 metabolites presented here shows potential to serve as a diagnostic tool, and future studies should target these metabolites in a clinical setting, in patients with non-specific symptoms and those with other cancer types, to evaluate their specificity towards glioma. Furthermore, the altered plasma metabolite levels are not proven here to be result of

glioma cancer cells, as the altered metabolite levels can equally be a result of cells in the microenvironment, or just an altered metabolism throughout the body as a consequence of disease progression. We recently showed that WHO classified subtypes of glioma tumors have different metabolic phenotypes that reaches beyond IDH-mutation status (24). A question that remains to be answered is if blood-based metabolomics can differentiate various molecular subtypes. Although we anticipate that our findings will greatly help to understand the mechanism of gliomagenesis and to find therapeutic targets, affected metabolic and biochemical pathways are still to be fully characterized before clinical applications can be developed.

Methods

Study Population and Nested Case-Control Design

We conducted a nested case-control study within two population-based prospective cohorts, NSHDS and EPIC. Detailed information about the cohorts is given in Supplemental Methods. Incident glioma cases in NHSDS (ICD-7, topography: 193, histology: 475-476) and EPIC (ICD-O-2, topography: C71, histology: 93800-94800) were identified via cancer registries or through active follow up. Each case was randomly paired with a matching control that at the time of diagnosis of the index case was alive and free of cancer (except non-melanoma skin cancer). Matching was based on sex, BMI, age (± six months), fasting status, time of sampling (± three months in NSHDS and ± one month in EPIC) and study center. In total, 1102 blood samples were included: 528 EDTA-plasma samples (264 pre-diagnostic glioma case samples and 264 control samples) from NSHDS and 574 sodium citrate plasma samples (287 pre-diagnostic glioma cases and 287 controls) from EPIC. The EPIC samples were from Spain, Italy, United Kingdom, the Netherlands, Germany and Norway. Additional information regarding the blood samples is given in Supplemental Methods. In this study, we used samples from the single-center NSHDS cohort for discovery and the multi-center EPIC cohort for validation.

Metabolomics Analyses

Metabolite analysis and data curation are described in detail in Supplemental Methods. We designed a constrained randomized run order (25), i.e. each case-control pair was run directly adjacent to each other in randomized order. All samples were analyzed using Metabolon Inc. global metabolomics platform, consisting

of four untargeted Ultrahigh Performance Liquid Chromatography-Tandem Mass Spectrometry (UHPLC-MS/MS) methods.

For targeted quantitative measurements of lactate, we used the LC-MS/MS-based Biocrates MxP500 quant platform and analyzed 354 NSHDS samples. This analysis is described in detail in Supplemental Methods.

Statistics

We analyzed matched case-control pairs as dependent samples throughout the study. For this purpose, an effect matrix with differences of relative concentrations for each metabolite of a case and its matched control was constructed. All statistical tests were two-sided, except for the one-sided hypergeometric test used in the metabolite enrichment analysis (Figure 7A-B and Table 3). $P<0.05$ was considered significant for all tests.

To get an overview of the samples, we performed Principal Component Analysis (PCA) (26), on case-control pairs from NSHDS and EPIC separately. One extreme outlier sample pair was observed in the PCA of NSHDS that indicated an abnormal plasma concentration difference within the pair, and was excluded from further data analysis, resulting in a final number of 550 cases and 550 controls. Furthermore, to get an overview of samples from both cohorts simultaneously, UMAP analysis was performed. UMAP plots were constructed for all samples, as individual observations, and for sample pairs using the effect matrix with calculated differences of matched case-control pairs.

To discover metabolites indicating glioma development, we performed multivariate modeling using OPLS-EP (25) with the effect matrix of case-control pairs from NSHDS and the curated metabolomics data of 1061 molecular features

(Supplemental Methods). Significance of OPLS-EP model was calculated using CV-ANOVA (two-sided) (27). Only metabolites in NSHDS that were multivariate significant (two-sided) (5, 28) were selected for validation in EPIC. For validation, the difference between cases and controls in metabolite levels towards diagnosis of the significant metabolites were examined in both NSHDS and EPIC. Metabolites that displayed the same direction towards diagnosis, with a mean difference of >10% closer to diagnosis (within 2 years and/or 1 year to diagnosis), were identified and examined on their ability to detect glioma development. The results were evaluated with ROC analyses. We calculated the AUC and the significance of the ROC curves using the Wilcoxon signed-rank test (two-sided). To assess if predictions were deviating depending on biological sex or glioma subtype, ROC analyses were done for females and males separately, and besides for all glioma also for glioblastoma and non-glioblastoma, separately (Supplemental Methods).

To put metabolites into biological context and to find altered metabolic pathways, we performed metabolite enrichment analysis using Metaboanalyst 5.0 (www.metaboanalyst.ca). For this analysis, we included metabolites within the curated NSHDS data set with known HMDB ID that were coherent with the Metaboanalyst database, in total 736 identified metabolites, as reference library. Hypergeometric test was used to calculate significance (one-sided).

Study approval

The Institutional Review Board of the International Agency for Research on Cancer and the local ethics committees approved the study. All participants provided written informed consent. All samples were pseudonymized and included in the study in accordance with the ethical standards of the Helsinki Declaration. This

project was approved by the ethical review board at Umeå University (Dnr 2017-295-31M).

Data availability

Data values associated with the manuscript and supplemental material shown in graphs are presented in the Supporting Data Values XLS file. The complete datasets generated for these analyses will be shared upon reasonable request to the corresponding authors: benny.bjorkblom@umu.se and beatrice.melin@umu.se. Data access requires ethical approval as existing informed consent will not permit personal data to be shared publicly. Requests will be reviewed by representatives of the NSHDS/EPIC steering committee.

Author contributions

Conceptualization: BM, BB; resources: UA, BM, RK, MBS, VP, IU, PA, SCY, MG, AKH, ACC, MJ; methodology: SL, BB, BM; data curation: SL, BB; formal analysis: SL, BB; validation: SL, BB; Interpretation of results: SL, BB, BM, HA; Visualizations: SL Writing – original draft: SL, BB; Writing – review and editing: SL, BB, BM, HA, LN; Input and valuable comments; RK, MBS, VP, IU, PA, SCY, MG, AKH, ACC, MJ. All authors read and approved the final manuscript.

Disclaimer

Where authors are identified as personnel of the International Agency for Research on Cancer / World Health Organization, the authors alone are responsible for the views expressed in this article and they do not necessarily represent the decisions, policy or views of the International Agency for Research on Cancer / World Health Organization.

Acknowledgement

We thank the Biobank Research Unit at Umeå University, Västerbotten Intervention Programme, the Northern Sweden MONICA study and Region Västerbotten for providing data and samples and acknowledge the contribution from Biobank Sweden, supported by the Swedish Research Council (VR 2017-00650). We acknowledge the use of data and biological samples from the following EPIC-cohorts: EPIC-Asturias cohort, PI J. Ramón Quirós; EPIC-Barcelona coordinating center, PI Antonio Agudo; EPIC-Granada cohort, PI Maria-José Sánchez; EPIC-Norrfolk, PI Nick Wareham; EPIC-Oxford, PI Tim Key; EPIC-Florence, PI Domenico Palli; EPIC-Ragusa, PI Rosario Tumino; EPIC-Turin, PI Carlotta Sacerdote; EPIC-Naples, PI Salvatore Panico; EPIC-Utrecht, PI Roel Vermeulen; and the National Institute for Public Health and the Environment (RIVM), Bilthoven, the Netherlands, for their contribution and ongoing support to the EPIC Study. In addition, we thank Pär Jonsson, Department of Chemistry, Umeå University, for data analysis consultation and Carl Wibom, Department of Radiation Sciences, Oncology, Umeå University, for metadata management.

This work was supported by Umeå University Hospital grant (7003839 to BM); the Swedish Research Council (2019-01566 to BM); the Swedish Cancer Society (CAN2018/390 to BM and 19 0370 to HA); the Cancer Research Foundation in Northern Sweden (AMP 21-1045, AMP22-1084 to SL); Lions Cancer Research Fund (LP21-2259 to BB); the Sjöberg Foundation (2020-01-07-08 to BM); and Health ministry support for early detection of Cancer (2020-2022 to BM).

The coordination of EPIC is financially supported by International Agency for Research on Cancer (IARC) and also by the Department of Epidemiology and Biostatistics, School of Public Health, Imperial College London which has additional

infrastructure support provided by the NIHR Imperial Biomedical Research Centre (BRC). The national cohorts are supported by: Danish Cancer Society (Denmark); Ligue Contre le Cancer, Institut Gustave Roussy, Mutuelle Générale de l'Education Nationale, Institut National de la Santé et de la Recherche Médicale (INSERM) (France); German Cancer Aid, German Cancer Research Center (DKFZ), German Institute of Human Nutrition Potsdam-Rehbruecke (DIfE), Federal Ministry of Education and Research (BMBF) (Germany); Associazione Italiana per la Ricerca sul Cancro-AIRC-Italy, Compagnia di SanPaolo and National Research Council (Italy); Dutch Ministry of Public Health, Welfare and Sports (VWS), Netherlands Cancer Registry (NKR), LK Research Funds, Dutch Prevention Funds, Dutch ZON (Zorg Onderzoek Nederland), World Cancer Research Fund (WCRF), Statistics Netherlands (The Netherlands); Health Research Fund (FIS) - Instituto de Salud Carlos III (ISCIII), Regional Governments of Andalucía, Asturias, Basque Country, Murcia and Navarra, and the Catalan Institute of Oncology - ICO (Spain); Swedish Cancer Society, Swedish Research Council and County Councils of Skåne and Västerbotten (Sweden); Cancer Research UK (14136 to EPIC-Norfolk; C8221/A29017 to EPIC-Oxford), Medical Research Council (1000143 to EPIC-Norfolk; MR/M012190/1 to EPIC-Oxford) (United Kingdom). Graphical abstract was created with BioRender.com.

References

1. Silvani A, et al. Malignant gliomas: early diagnosis and clinical aspects. *Neurol Sci.* 2011;32:S207-S208.
2. Nava F, et al. Survival effect of first- and second-line treatments for patients with primary glioblastoma: a cohort study from a prospective registry, 1997-2010. *Neuro Oncol.* 2014;16(5):719-727.
3. The Brain Tumor Charity. Finding a better way? Improving the quality of life for people affected by brain tumours. Published 2013. https://www.basw.co.uk/system/files/resources/basw_21512-10_0.pdf Accessed June 17, 2022.
4. Körber V, et al. Evolutionary Trajectories of IDHWT Glioblastomas Reveal a Common Path of Early Tumorigenesis Instigated Years ahead of Initial Diagnosis. *Cancer Cell.* 2019;35(4):692-704.
5. Jonsson P, et al. Identification of Pre-Diagnostic Metabolic Patterns for Glioma Using Subset Analysis of Matched Repeated Time Points. *Cancers.* 2020;12(11).
6. Björkblom B, et al. Metabolomic screening of pre-diagnostic serum samples identifies association between alpha- and gamma-tocopherols and glioblastoma risk. *Oncotarget.* 2016;7(24):37043-37053.
7. Beyoglu D, and Idle JR. Metabolic Rewiring and the Characterization of Oncometabolites. *Cancers.* 2021;13(12).
8. Nothern Sweden Health and Disease Study, NSHDS. https://www.umu.se/en/biobank-research-unit/provsamlingar-och-register/northern-sweden-health-and-disease-study-vip-monica-and-the-mammography-screening-project/ Accessed June 17, 2022.
9. Riboli E, et al. European prospective investigation into cancer and nutrition (EPIC): study populations and data collection. *Public Health Nutr.* 2002;5(6b):1113-1124.
10. Khadka M, et al. The Effect of Anticoagulants, Temperature, and Time on the Human Plasma Metabolome and Lipidome from Healthy Donors as Determined by Liquid Chromatography-Mass Spectrometry. *Biomolecules.* 2019;9(5).
11. Sotelo-Orozco J, et al. A Comparison of Serum and Plasma Blood Collection Tubes for the Integration of Epidemiological and Metabolomics Data. *Front Mol Biosci.* 2021;8.

12. Carayol M, et al. Reliability of Serum Metabolites over a Two-Year Period: A Targeted Metabolomic Approach in Fasting and Non-Fasting Samples from EPIC. *Plos One*. 2015;10(8).
13. Vaupel P, et al. The Warburg effect: essential part of metabolic reprogramming and central contributor to cancer progression. *Int J Radiat Biol*. 2019;95(7):912-919.
14. Bi JF, et al. Altered cellular metabolism in gliomas - an emerging landscape of actionable co-dependency targets. *Nat Rev Cancer*. 2020;20(1):57-70.
15. Jansen RS, et al. N-lactoyl-amino acids are ubiquitous metabolites that originate from CNDP2-mediated reverse proteolysis of lactate and amino acids. *P Natl Acad Sci USA*. 2015;112(21):6601-6606.
16. Morville T, et al. Plasma Metabolome Profiling of Resistance Exercise and Endurance Exercise in Humans. *Cell Rep*. 2020;33(13).
17. Li VL, et al. An exercise-inducible metabolite that suppresses feeding and obesity. *Nature*. 2022;606(7915):785-790.
18. Wu WYY, et al. Pre-diagnostic levels of sVEGFR2, sTNFR2, sIL-2R alpha and sIL-6R are associated with glioma risk: A nested case-control study of repeated samples. *Cancer Med-Us*. 2022;11(4):1016-1025.
19. Dorochow E, et al. Metabolic Profiling in Rheumatoid Arthritis, Psoriatic Arthritis, and Psoriasis: Elucidating Pathogenesis, Improving Diagnosis, and Monitoring Disease Activity. *J Pers Med*. 2022;12(6).
20. Fernstrom JD, and Fernstrom MH. Tyrosine, phenylalanine, and catecholamine synthesis and function in the brain. *J Nutr*. 2007;137(6):1539s-1547s.
21. Swift CC, et al. Updates in Diagnosis, Management, and Treatment of Neuroblastoma. *Radiographics*. 2018;38(2):566-580.
22. Gonzalez-Riano C, et al. Prognostic biomarkers of Parkinson's disease in the Spanish EPIC cohort: a multiplatform metabolomics approach. *Npj Parkinsons Dis*. 2021;7(1).
23. Shea D, et al. SOBA: Development and testing of a soluble oligomer binding assay for detection of amyloidogenic toxic oligomers. *Proc Natl Acad Sci U S A*. 2022;119(50):e2213157119.
24. Björkblom B, et al. Distinct metabolic hallmarks of WHO classified adult glioma subtypes. *Neuro-Oncology*. 2022;24(9):1454-1468.

25. Jonsson P, et al. Constrained randomization and multivariate effect projections improve information extraction and biomarker pattern discovery in metabolomics studies involving dependent samples. *Metabolomics*. 2015;11(6):1667-1678.

26. Wold S, et al. Principal Component Analysis. *Chemometr Intell Lab*. 1987;2(1-3):37-52.

27. Eriksson L, et al. CV-ANOVA for significance testing of PLS and OPLS (R) models. *J Chemometr*. 2008;22(11-12):594-600.

28. Jonsson P, et al. Statistical loadings and latent significance simplify and improve interpretation of multivariate projection models. *bioRxiv*. 2018.

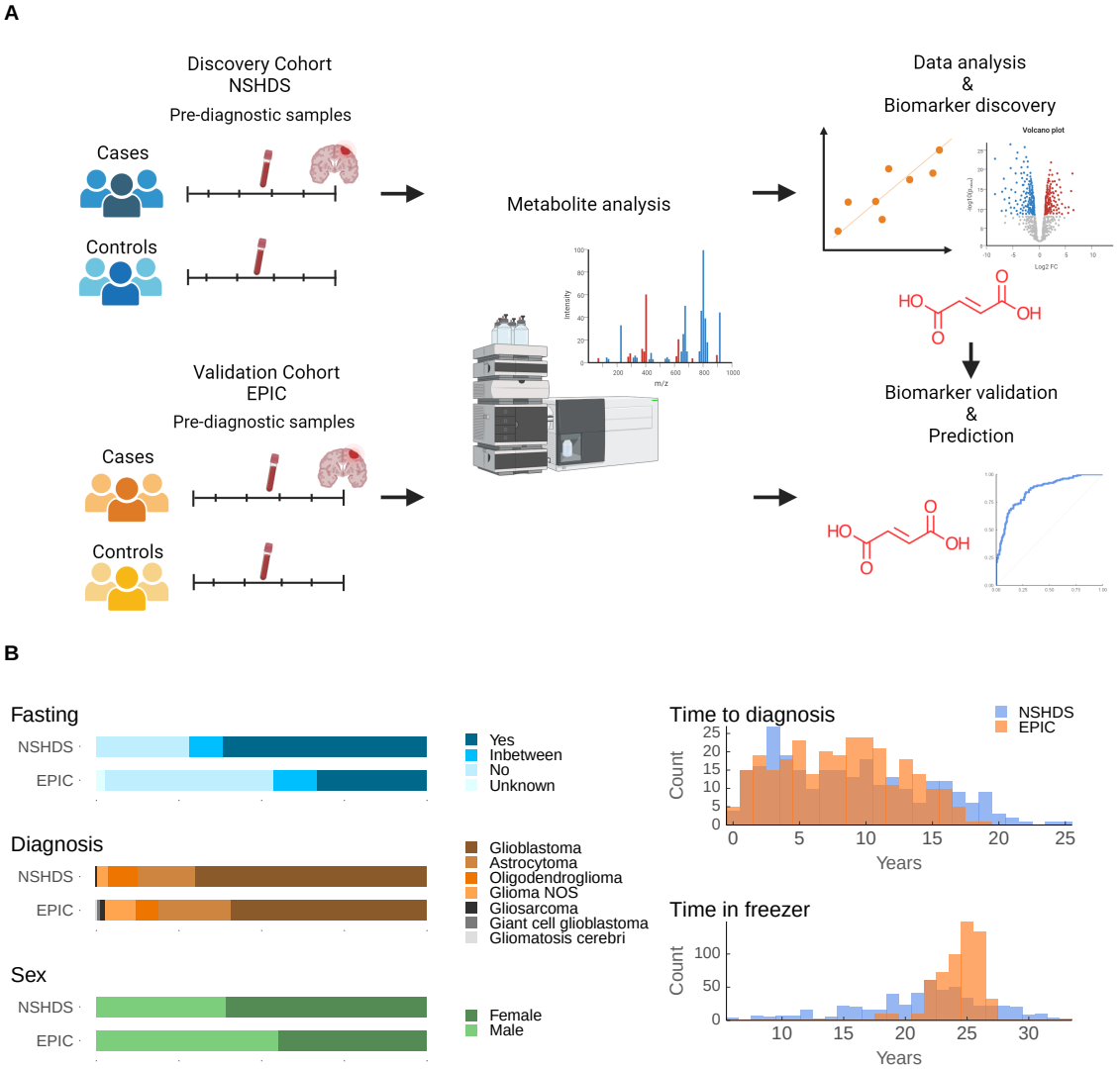

Figure 1. Study overview. (A) Overview of study design and workflow. Illustrations were created with BioRender.com. (B) Overview of cohort characteristics for NSHDS and EPIC samples.

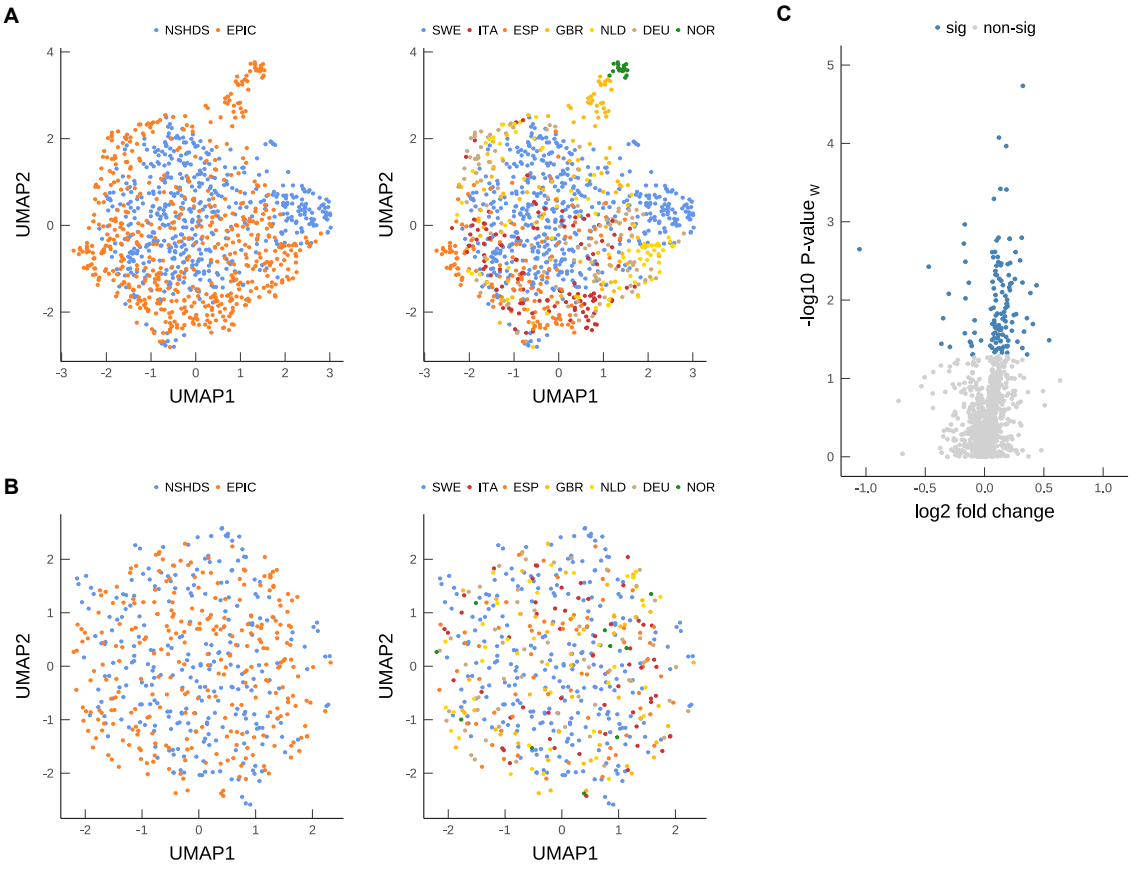

Figure 2. Data overview. (A and B) UMAP plots of plasma samples from NSHDS and EPIC. A. Cases and controls (n=1100) colored by cohort (left) and sampling country (right). B. Matched case-control pairs (n=550) colored by cohort (left) and sampling country (right). SWE = Sweden; ITA = Italy; ESP = Spain; GBR = United Kingdom; NLD = Netherlands; DEU = Germany; NOR = Norway. (C) Volcano plot of detected molecular features in NSHDS within eight years to diagnosis (n=130 case-control pairs), with effect sizes and significance levels for each of the 1061 molecular features as log-ratios. Significance was calculated by multivariate significance (two-sided, P-valuew plotted). Sig = Significant molecular features; non-sig = non-significant molecular features.

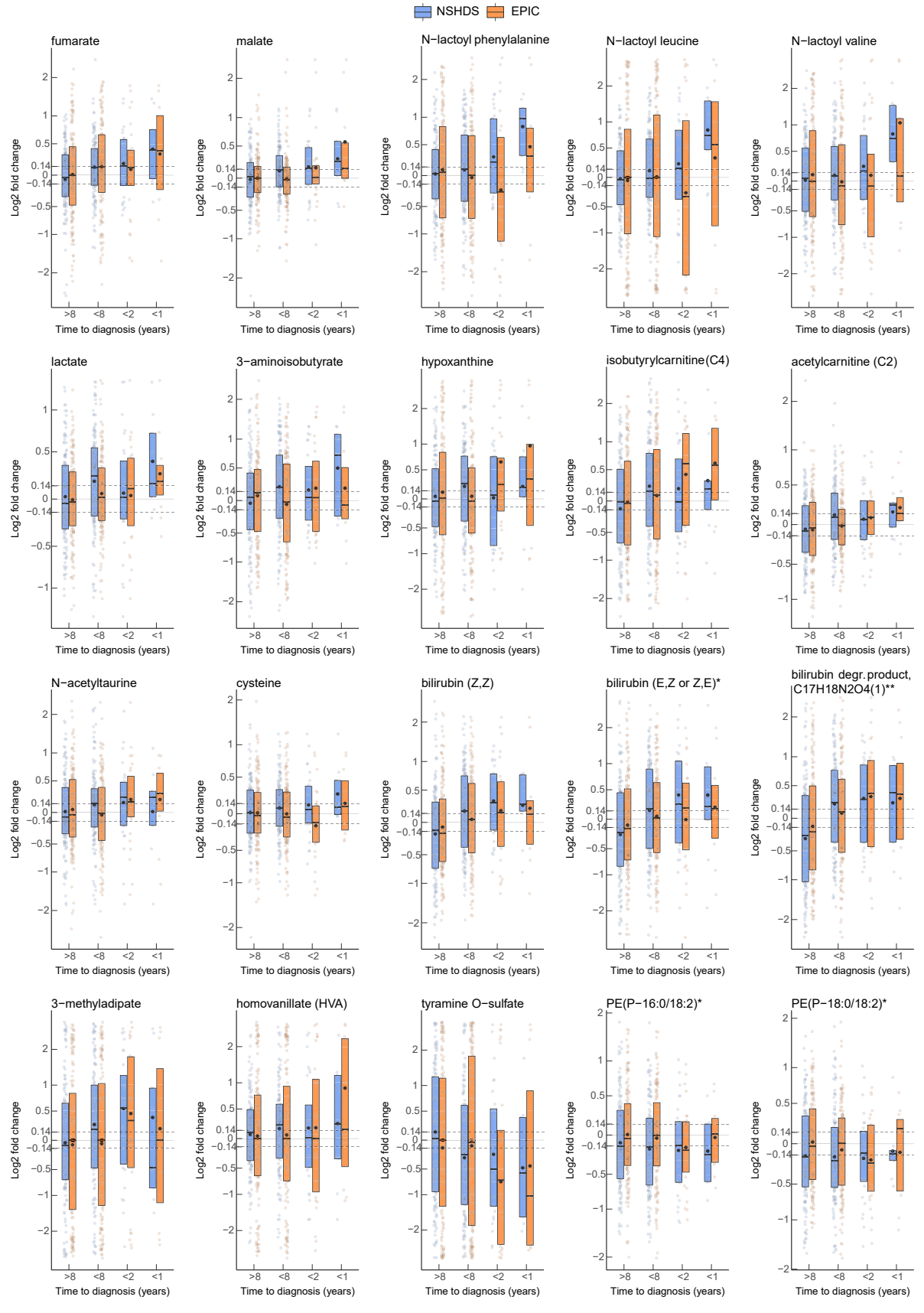
NSHDS
EPIC
fumarate
malate
N−lactoyl phenylalanine
N−lactoyl leucine
N−lactoyl valine
lactate
3−aminoisobutyrate
hypoxanthine
isobutyrylcarnitine(C4)
acetylcarnitine (C2)
N−acetyltaurine
cysteine
bilirubin (Z,Z)
bilirubin (E,Z or Z,E)*
bilirubin degr.product, C17H18N2O4(1)**
3−methyladipate
homovanillate (HVA)
tyramine O−sulfate
PE(P−16:0/18:2)*
PE(P−18:0/18:2)*
Log2 fold change
Time to diagnosis (years)
>8
<8
<2
<1

Figure 3. Metabolite levels for case-control pairs towards diagnosis. Boxplots with average (dot) and median (line) fold change in case-control pairs for NSHDS (blue) and EPIC (orange) samples, subgrouped according to time to diagnosis (>8 years: NSHDS, n=133 and EPIC, n=148. <8 years: NSHDS, n=130 and EPIC, n=139. <2 years: NSHDS, n=28 and EPIC, n=28. <1 year: NSHDS, n=9 and EPIC, n=11). Dashed horizontal lines display a 10% difference. The Y-axis is non-linearly transformed. All metabolite identifications were validated using synthetic standards, except putative identifications denoted * or **.

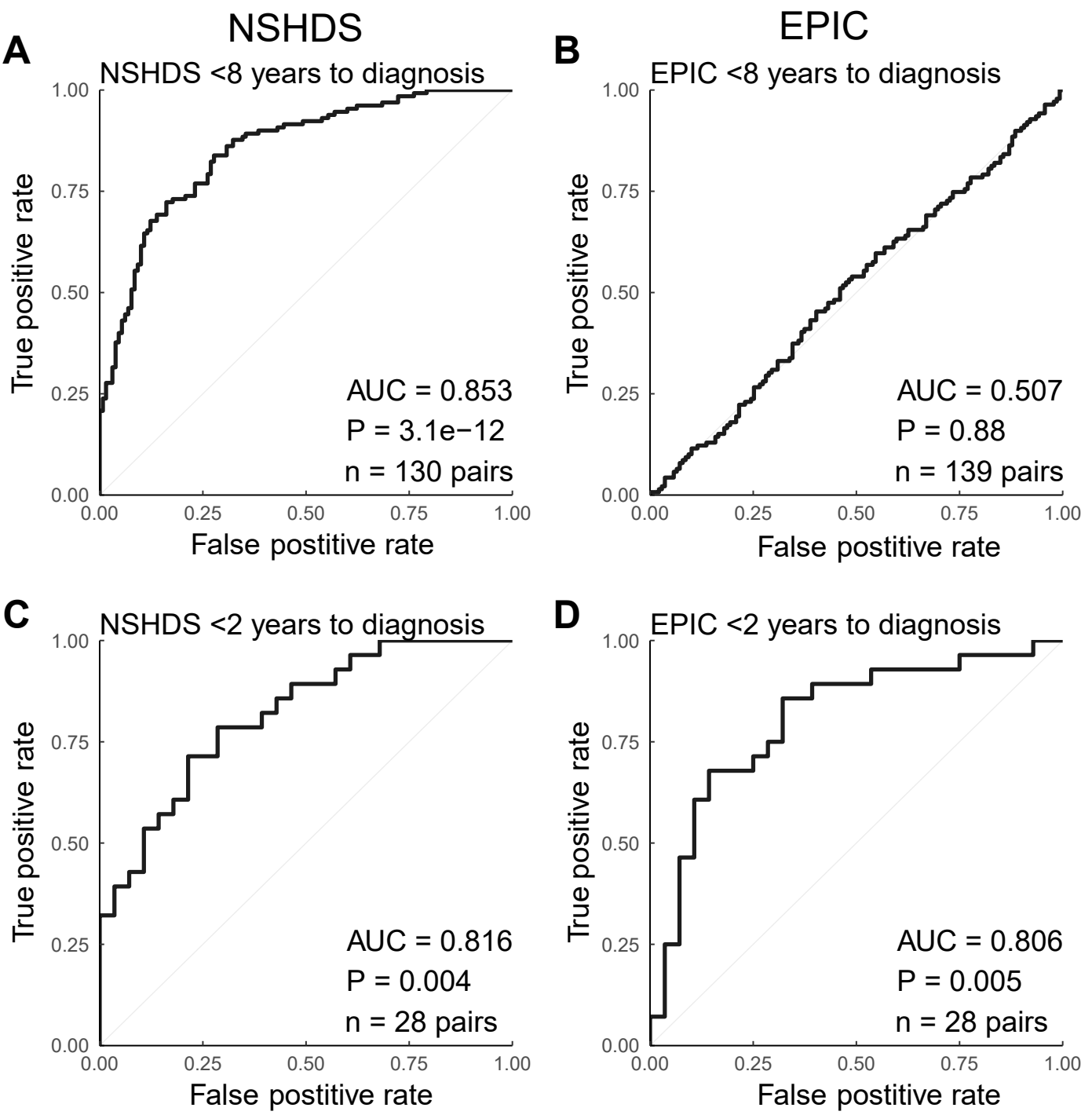

Figure 4. ROC analysis using a panel of 20 metabolites. Glioma case-control pairs sampled less than eight years before diagnosis in (A) NSHDS and (B) EPIC, and less than two years before diagnosis in (C) NSHDS and (D) EPIC. Wilcoxon signed-rank test (two-sided) was used to calculate the significance of the ROC curves. n = number of pairs available for each analysis.

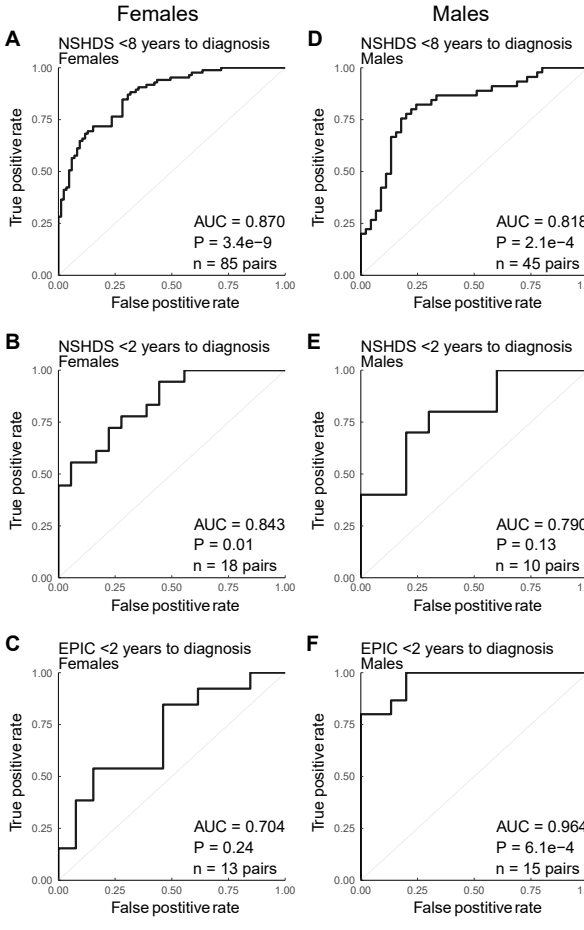

Figure 5. ROC analysis using a panel of 20 metabolites for females and males. (A and B) NSHDS female case-control pairs sampled less than eight years (A) or less than two years (B) before diagnosis. (C) EPIC female case-control pairs sampled less than two years before diagnosis. (D and E) NSHDS male case-control pairs sampled less than eight years (D) or less than two years (E) before diagnosis. (F) EPIC male case-control pairs sampled less than two years before diagnosis. Wilcoxon signed-rank test (two-sided) was used to calculate the significance of the ROC curves. n = number of pairs available for each analysis.

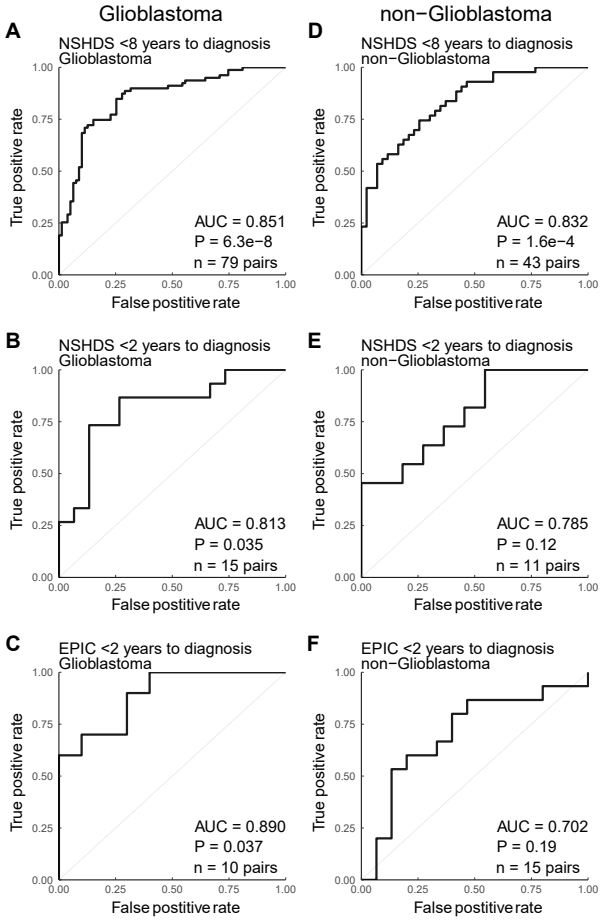

Figure 6. ROC analysis using a panel of 20 metabolites on glioma subtypes. (A and B) NSHDS glioblastoma case-control pairs sampled less than eight years (A) or less than two years (B) before diagnosis. (C) EPIC glioblastoma case-control pairs sampled less than two years before diagnosis. (D and E) NSHDS non-glioblastoma case-control pairs sampled less than eight years (D) or less than two years (E) before diagnosis. (F) EPIC non-glioblastoma case-control pairs sampled less than two years before diagnosis. Wilcoxon signed-rank test (two-sided) was used to calculate the significance of the ROC curves. n = number of pairs available for each analysis.

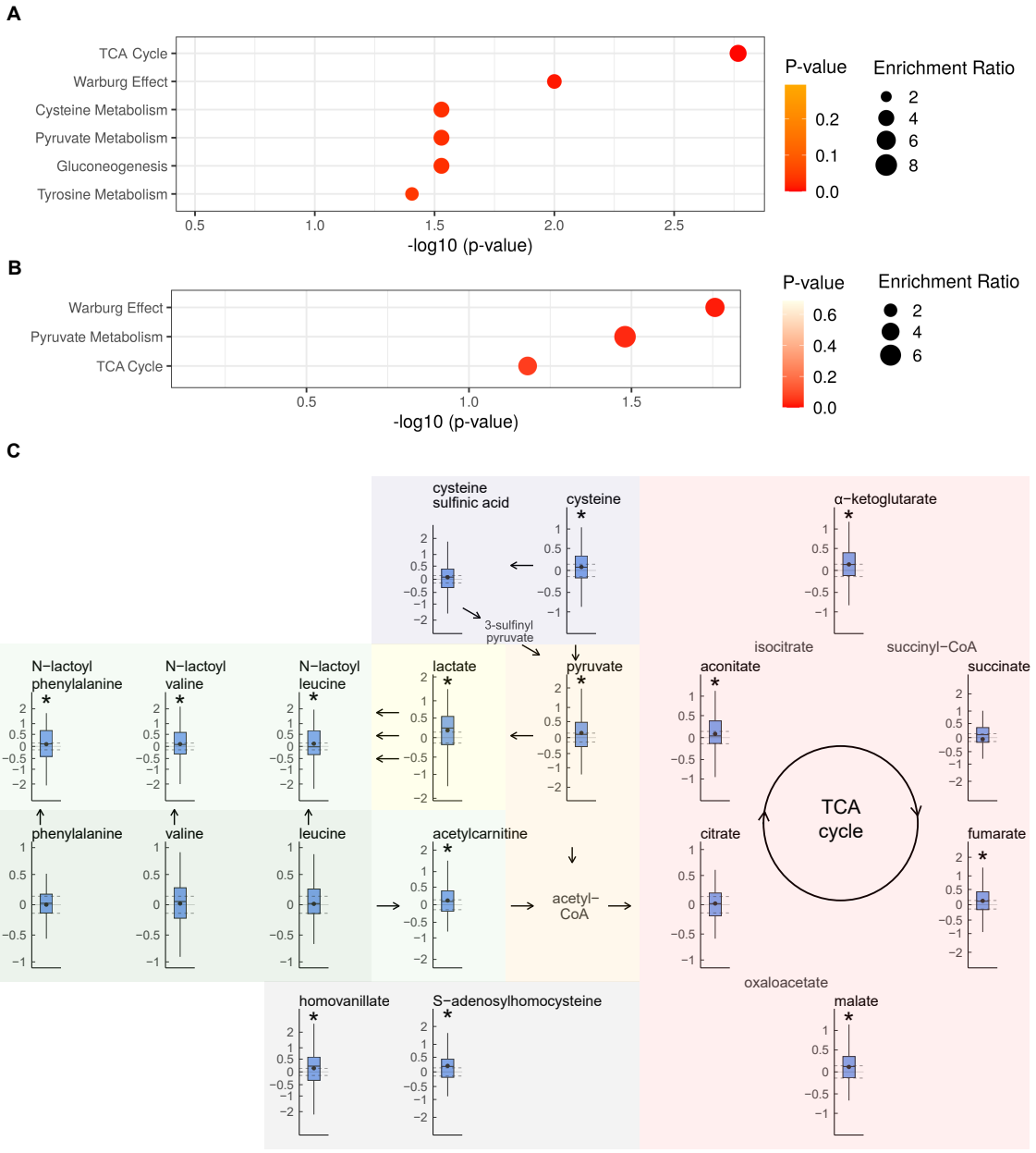

Figure 7. Overview of significant metabolic pathways. (A and B) Pathway enrichment analysis using (A) the 93 metabolites significant within eight years to diagnosis in NSHDS (B) the panel of 20 metabolites in common for NSHDS and EPIC. Hypergeometric test was used to calculate significance (one-sided). (C) Scheme of detected metabolites present in the TCA cycle, the Warburg effect, gluconeogenesis, pyruvate-, cysteine- and tyrosine metabolism, and neighboring amino acid metabolism. Boxplots with average (dot) and median (line) log2 fold change are presented from case-control pairs within eight years to diagnosis from NSHDS (n=130). Dashed horizontal lines display a 10% difference. Significant metabolites, calculated by multivariate significance (two-sided), are denoted with *. Undetected pathway metabolites are included with name without boxplot.

Table 1. Demographics for NSHDS and EPIC cohort participants. All participants, and subgrouped according to time to diagnosis.

NSHDS	**All years**		**>8 years to diagnosis**		**<8 years to diagnosis**		**<2 years to diagnosis**	
	Cases	Controls	Cases	Controls	Cases	Controls	Cases	Controls
Subjects, n	263	263	133	133	130	130	28	28
Sex, n (%)								
Male	103 (39.2)	103 (39.2)	58 (43.6)	58 (43.6)	45 (34.6)	45 (34.6)	10 (35.7)	10 (35.7)
Female	160 (60.8)	160 (60.8)	75 (56.4)	75 (56.4)	85 (65.4)	85 (65.4)	18 (64.3)	18 (64.3)
Age at diagnosis (years), mean (range)	62.5 (32.5-80.0)	n/a	66.8 (41.5-80.0)	n/a	58.2 (32.5-77.3)	n/a	54.6 (32.5-67.6)	n/a
Age at sample collection (years), mean (range)	53.7 (28.6-73.6)	53.7 (27.8-73.0)	53.2 (29.4-68.8)	53.2 (30.1-68.5)	54.2 (28.6-73.6)	54.2 (27.8-73.0)	53.4 (30.5-66.4)	53.3 (30.4-66.6)
Time to diagnosis (years), mean (range)	8.8 (0.15-25.1)	n/a	13.6 (8.02-25.1)	n/a	3.9 (0.15-7.98)	n/a	1.2 (0.15-1.97)	n/a
Sampling date (year), median (range)	1998 (1986-2014)	1998 (1986-2014)	1996 (1986-2008)	1996 (1986-2008)	1999 (1988-2014)	1999 (1988-2014)	2001 (1991-2014)	2001 (1991-2014)
Time in freezer (years), mean (range)	21.4 (5.8-33.3)	21.5 (5.9-33.2)	23.4 (11.7-33.3)	23.4 (11.9-33.2)	19.5 (5.8-31.3)	19.5 (5.9-31.3)	18.0 (5.9-28.2)	18.0 (5.9-28.2)
BMI (kg/m^2), mean (range)	25.8 (18.3-39.8)	25.4 (18.1-35.0)	26.0 (18.8-37.3)	25.5 (18.7-33.5)	25.7 (18.3-39.8)	25.3 (18.1-35.0)	25.7 (18.3-35.1)	25.9 (18.1-31.9)
Fasting status, n								
0-4 h	74	75	32	30	42	45	13	13
4-8 h	27	26	16	18	11	8	2	2
>8 h	162	162	85	85	77	77	13	13
Glioma subtype, n								
Glioblastoma: 9440/3	184	n/a	105	n/a	79	n/a	15	n/a
Gliosarcoma: 9442/3	1	n/a	0	n/a	1	n/a	0	n/a
Astrocytoma: 9400/3, 9401/3	46	n/a	19	n/a	27	n/a	7	n/a
Oligodendroglioma: 9450/3, 9451/3	24	n/a	8	n/a	16	n/a	4	n/a
Glioma NOS: 9380/3	8	n/a	1	n/a	7	n/a	2	n/a

Continuation of Table 1.

EPIC	**All years**		**>8 years to diagnosis**		**<8 years to diagnosis**		**<2 years to diagnosis**	
	Cases	Controls	Cases	Controls	Cases	Controls	Cases	Controls
Subjects, n	287	287	148	148	139	139	28	28
Sex, n (%)								
Male	129 (44.9)	129 (44.9)	63 (42.6)	63 (42.6)	66 (47.5)	66 (47.5)	15 (53.6)	15 (53.6)
Female	158 (55.1)	158 (55.1)	85 (57.4)	85 (57.4)	73 (52.5)	73 (52.5)	13 (46.4)	13 (46.4)
Country								
Italy	57	57	33	33	24	24	5	5
Spain	71	71	48	48	23	23	3	3
United Kingdom	52	52	28	28	24	24	4	4
The Netherlands	41	41	19	19	22	22	7	7
Germany	56	56	18	18	38	38	7	7
Norway	10	10	2	2	8	8	2	2
Age at diagnosis (years), mean (range)	62.5 (26.8-85.0)	n/a	66.1 (41.1-85.0)	n/a	58.9 (26.8-80.6)	n/a	54.2 (33.3-70.8)	n/a
Age at sample collection (years), mean (range)	54.4 (24.3-74.6)	54.4 (23.5-73.8)	54.2 (33.0-71.4)	54.2 (32.8-71.0)	54.7 (24.3-74.6)	54.6 (23.5-73.8)	53.0 (32.7-70.4)	53.0 (32.5-69.9)
Time to diagnosis (years), mean (range)	8.1 (0.22-18.6)	n/a	11.8 (8.1-18.6)	n/a	4.3 (0.22-7.95)	n/a	1.2 (0.22-1.96)	n/a
Sampling date (year), median (range)	1995 (1992-2002)	1995 (1992-2002)	1995 (1992-2001)	1995 (1992-2001)	1995 (1993-2002)	1995 (1993-2002)	1995 (1994-2001)	1995 (1993-2001)
Time in freezer (years), mean (range)	24.2 (17.7-27.1)	24.2 (17.8-27.2)	24.7 (18.1-27.1)	24.7 (18.2-27.2)	23.8 (17.7-26.8)	23.8 (17.8-26.9)	23.8 (18.3-26.0)	23.8 (18.3-26.1)
Fasting status, n								
0-3 h	145	149	67	69	78	80	16	17
3-6 h	38	37	19	18	19	19	5	5
>6 h	95	95	57	57	38	38	6	6
Unknown	9	6	5	4	4	2	1	0
Glioma subtype, n								
Glioblastoma: 9440/3	170	n/a	100	n/a	70	n/a	10	n/a
Giant cell glioblastoma: 9441/3	2	n/a	1	n/a	1	n/a	0	n/a
Gliosarcoma: 9442/3	5	n/a	3	n/a	2	n/a	1	n/a
Astrocytoma: 9400/3, 9401/3, 9411/3, 9420/3	63	n/a	25	n/a	38	n/a	11	n/a
Oligodendroglioma: 9450/3, 9451/3	20	n/a	10	n/a	10	n/a	4	n/a
Glioma NOS: 9380/3	26	n/a	9	n/a	17	n/a	2	n/a
Gliomatosis cerebri: 9381/3	1	n/a	0	n/a	1	n/a	0	n/a

.

Table 2. List of 20 significant metabolites discovered in NSHDS with the same progression pattern towards diagnosis in the EPIC validation cohort.

Metabolites	P-value	Mean % difference	HMDB ID	Sub-pathway	Super pathway
Higher in cases					
lactate	0.0004	14	HMDB0000190	Glycolysis, Gluconeogenesis, and Pyruvate Metabolism	Carbohydrate
acetylcarnitine (C2)	0.0016	9	HMDB0000201	Fatty Acid Metabolism (Acyl Carnitine, Short Chain)	Lipid
hypoxanthine	0.0017	16	HMDB0000157	Purine Metabolism, (Hypo)Xanthine/Inosine containing	Nucleotide
malate	0.0028	8	HMDB0000156	TCA Cycle	Energy
fumarate	0.0054	9	HMDB0000134	TCA Cycle	Energy
bilirubin degradation product, C17H18N2O4 (1)**	0.0062	16		Partially Characterized Molecules	Partially Characterized Molecules
3-aminoisobutyrate	0.0069	16	HMDB0002166	Pyrimidine Metabolism, Thymine containing	Nucleotide
homovanillate (HVA)	0.014	12	HMDB0000118	Tyrosine Metabolism	Amino Acid
3-methyladipate	0.015	20	HMDB0000555	Fatty Acid, Dicarboxylate	Lipid
bilirubin (Z,Z)	0.016	13	HMDB0000054	Hemoglobin and Porphyrin Metabolism	Cofactors and Vitamins
isobutyrylcarnitine (C4)	0.019	17	HMDB0000736	Leucine, Isoleucine and Valine Metabolism	Amino Acid
N-lactoyl phenylalanine	0.026	6	HMDB0062175	Phenylalanine Metabolism	Amino Acid
cysteine	0.027	5	HMDB0000574	Methionine, Cysteine, SAM and Taurine Metabolism	Amino Acid
N-lactoyl leucine	0.03	8	HMDB0062176	Leucine, Isoleucine and Valine Metabolism	Amino Acid
N-acetyltaurine	0.041	9	HMDB0240253	Methionine, Cysteine, SAM and Taurine Metabolism	Amino Acid
bilirubin (E,Z or Z,E)*	0.042	11	HMDB0000488	Hemoglobin and Porphyrin Metabolism	Cofactors and Vitamins
N-lactoyl valine	0.043	7	HMDB0062181	Leucine, Isoleucine and Valine Metabolism	Amino Acid
Lower in cases					
PE(P-16:0/18:2)*	0.0019	-13	HMDB0011343	Plasmalogen	Lipid
tyramine O-sulfate	0.0083	-23	HMDB0006409	Tyrosine Metabolism	Amino Acid
PE(P-18:0/18:2)*	0.0095	-12	HMDB0011376	Plasmalogen	Lipid

P-values and mean percentage difference were calculated from case-control pairs within eight years to diagnosis in NSHDS (n=130). Significance levels were calculated by multivariate significance using loadings w and p (two-sided, P-value w presented) (5, 28). * and ** denotes metabolites with putative identifications.

Table 3. List of overrepresented significant metabolites and the metabolic pathways they are predominantly related to.

Pathway	TCA cycle	Warburg effect	Cysteine metabolism	Pyruvate metabolism	Gluconeogenesis	Tyrosine metabolism
Significant metabolites	aconitate α-ketoglutarate fumarate malate pyruvate	α-ketoglutarate fumarate lactate malate pyruvate	α-ketoglutarate cysteine pyruvate	lactate malate pyruvate	α-ketoglutarate lactate pyruvate	α-ketoglutarate fumarate homovanillate S-adenosylhomo-cysteine
Number of metabolites detected for each pathway	10	14	7	7	7	13
P-value	0.002	0.01	0.03	0.03	0.03	0.04

Hypergeometric test was used to calculate significance (one-sided).